LUND UNIVERSITY

Statistical analysis of measured short-term impulse response functions of 1.88 GHz radio channels in Stockholm with corresponding channel model

Alayon Glazunov, Andres; Asplund, Henrik; Berg, Jan-Erik

Link to publication

Statistical analysis of measured short-term impulse response functions of 1.88 GHz radio channels in Stockholm with corresponding channel model

Andres Alayon Glazunov, Henrik Asplund, Jan-Erik Berg

Ericsson Radio Systems AB
Ericsson Research
S-164 80 Stockholm, Sweden
Givenname.Surname@era-t.ericsson.se

Abstract: *A statistical analysis of amplitudes corresponding to multipath components in outdoor (urban/suburban) channels is presented. The study is based on short-term complex impulse response measurements conducted in Stockholm at 1.88 GHz carrier frequency with 5MHz bandwidth. The actual investigations show that the Rice distribution gives the best fitting in the Kramer-von-Mises sense. Further it is shown that in average the strongest tap fades less than the other taps in the impulse response. A global average model was devised for the power delay profile and corresponding Rice K-factor.*

1 Introduction

The time-dispersive character of the radio channel together with its variability set constraints on the performance of a mobile communication system. Therefore, in order to design communication systems capable of providing high-quality services, reliable channel models have to lie as a ground for such a system. Numerous wideband channel models have appeared during last years, among others [1-3]. A widely used approach introduced by Turin [1], models the complex impulse response (CIR), as a result of multipath propagation by means of a linear filter:

$$h(\tau, t) = \sum_k a_k(t)\exp(j\theta_k(t))\delta(\tau - \tau_k) \quad (1.1)$$

where a_k is the real amplitude of the k-th multipath component arriving at time delay τ_k, and θ_k is the corresponding phase shift assumed uniformly distributed over [0, 2π]. On the other hand, the amplitude a_k is usually assumed Rayleigh, Rice, Nakagami or Lognormal depending on the propagation scenario.

However direct evidence for the statistical behavior of the multipath components has not been found in literature except for the statistical description of signal envelopes at a few time delays or with other words for a few multipath components [4].

The aim of the actual paper is to give a better insight into the statistics of the fading behavior of the multipath components in short-term CIR in Urban and Suburban propagation areas. The analysis is based on wideband channel impulse response measurements in Stockholm City and in a Stockholm suburb, performed at the 1.88 GHz band. Some earlier results based on the same measurement campaign were presented in [5].

2 Measurements

Two areas were chosen for the measurements. The first one, Kista-Sollentuna, was situated outside the city borders and can be denoted as a mixture of Urban and Suburban areas. There, measurements at 30 locations were performed covering mobile-base distances from 200 m to 2 km. The second campaign that covered distances from 150 m to 2.5 km, was conducted in some central parts of Stockholm city. In both occasions the base station antenna was located at approximately 25 m above ground, while the mobile antenna was placed on top of a van.

A 511 bit PN-sequence was transmitted at the base station position. At the mobile, data was gathered with sampling rate of 6.4 MHz by means of a Vector Signal Analyzer. Each measured short-term CIR comprised 1430 instantaneous CIR of 109 µs length. Each measurement covered approximately 0.15 seconds (1 to 4 m depending on the speed of the mobile) along the mobile path. By signal post-processing 5MHz channel versions were extracted from the raw data. To achieve a further improvement of the dynamic range, besides the signal post-processing applied to measured CIR in [5], Doppler filtering of the measured data was implemented using a 4th order low-pass digital Butterworth filter with the cut-off frequency equal to the maximum Doppler frequency. Fig. 1 shows the average Power Delay Profile (PDP), as computed before the Doppler filtering (thin solid line) and after (thick solid line).
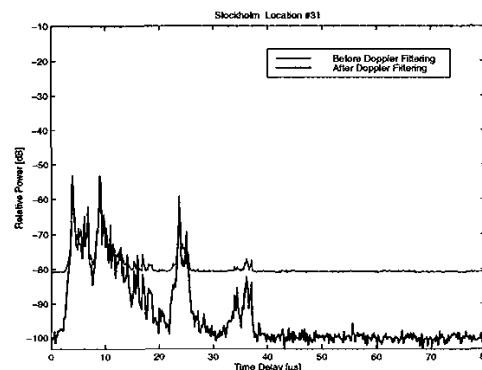

Figure 1. Power Delay Profile of an impulse response measured in the Stockholm area.

As is clear from the plots the PDP computed after the filtering gives a more detailed picture of the propagation environment. Scatterers "drowned" under the noise level

are now "visible" and the cluster nature of the observed profiles more clear.

The dynamic range of the PDPs is improved by removing the high frequency components outside the Doppler interval, and more correct conclusions can be drawn from estimated statistical behavior of the multipath components.

3 Multipath Amplitude Distribution

In this section the distribution of the multipath amplitudes a_k (see equation 1.1) is studied by estimating the envelope of the measured complex channel impulse response $|h(\tau_k,t)|$. It is well known that fading variation of a single multipath component is determined by the propagation environment, more specifically by the objects (buildings, mountains, lakes, vegetation and of course people) surrounding both the mobile and the base stations. So, depending on the environment, the character of the fading variation of the measured signals will change. Most common distributions found in literature, used to describe the rapid fading variations, are the Rayleigh, Rice, Nakagami, Weibull and Lognormal distributions [6-9]. Therefore they have been chosen as candidates to model the amplitude variations of taps in the PDP.

The probability density function (pdf) corresponding to the distributions are listed in Table 1 together with the distribution parameters. The Rayleigh distribution is usually used to describe the local area variations of signals composed by a large number of partial waves of quite similar amplitudes that corresponds to the no-line-of-sight situation with $2\sigma^2$ being the average power. The Rice distribution, on the other hand, describes the situation when a dominant path with power amplitude s^2, that can be a direct or a reflected wave, is added to a diffuse scattering process with power $2\sigma^2$. The Rice distribution contains the Rayleigh as a special case when no dominant path is present ($s=0$). $I_0(.)$ is the zero-th order modified Bessel function of first kind. The Rice distribution is often characterized by the K-factor that is defined as the ratio of the power of the direct path component s^2 and the random one $2\sigma^2$, $K=s^2/2\sigma^2$($K \geq 0$). In the present paper we decided to first compute parameters s and σ deriving the K-factor afterwards.

The next candidate is the Nakagami distribution and is also specified in terms of two parameters, the mean power Ω and the m-factor ($m > 0.5$). In general the Nakagami and Rice distributions can be explained by equivalent models [9]. The Nakagami distribution with $m = 1$ reduces to the Rayleigh distribution or equivalent Rice with $K=0$.

Further we have the Weibull distribution with shape parameter $\alpha > 0$ and the scale parameter $\beta > 0$.

The last considered distribution is the Lognormal, characterized by the shape parameter $\sigma > 0$ and the scale

parameter $\mu \in (-\infty,\infty)$.

The parameters of the theoretical distributions shown in Table 1 have been derived using the Maximum Likelihood Estimator approach (MLE) [10]. The MLEs for the Weibull and Nakagami distribution are also given in [10]. The derivation of MLEs for the Rayleigh, Rice and Nakagami distributions are given in Appendix A.

In order to estimate the goodness-of-fit of the rivalling distributions the Cramer-von-Mises criterion [11] was chosen. This criterion states that a good fit of an empirical cumulative distribution function (cdf) $F'_R(r)$ to a theoretical cdf $F_R(r)$ is obtained for a low value of the curve fitting error ε^2 given by the following integral:

$$\varepsilon^2 = \int_{-\infty}^{\infty} [F_R(r) - F'_R(r)]^2 p_R(r) dr \qquad (3.1)$$

As is clear from equation (3.1) the tails of the probability distributions are weighted less than the region around the most probable values.

Distribution and parameters	Probability Density Function (PDF)
Rayleigh σ	$p_R(r) = \dfrac{r}{\sigma^2} e^{-\frac{r^2}{2\sigma^2}}$
Rice s, σ	$p_R(r) = \dfrac{r}{\sigma^2} e^{-\frac{r^2+s^2}{2\sigma^2}} I_0(\frac{rs}{\sigma^2})$
Nakagami m, Ω	$p_R(r) = \dfrac{2m^m r^{2m-1}}{\Gamma(m)\Omega^m} e^{-\left(\frac{m}{\Omega}\right)r^2}$
Weibull α, β	$p_R(r) = \alpha\beta^{-\alpha}r^{\alpha-1} e^{-\left(\frac{r}{\beta}\right)^\alpha}$
Lognormal μ, σ	$p_R(r) = \dfrac{1}{r\sqrt{2\pi\sigma^2}} e^{-\frac{(\ln(r)-\mu)^2}{2\sigma^2}}$

Table 1   Probability Density Functions.

3.1 Parameter estimates and goodness-of-fit test results

As mentioned above, the distribution of individual multipath components were analyzed. Theoretical Rayleigh, Rice, Nakagami, Weibull and Lognormal pdf's (see Table 1) were fitted to empirical distributions. Parameters for the theoretical distribution functions were estimated from the empirical data by means of Maximum Likelihood Estimator approach.

The analyzed data was divided in two sets. To the first one belong 30 measurements in Kista-Sollentuna, the second one consists of 41 measurements carried out in

Stockholm city[5].

In Fig. 2 the results for the frequency of best fitting in percents for the considered theoretical distributions are shown. Results from Kista-Sollentuna (Stockholm suburb) are given for the 5 MHz channels. As the color of columns goes from black to white (gray scale) the "fitting quality" goes from best to worst. The height of the columns corresponds to the frequency of best fitting, second best fitting and so on.
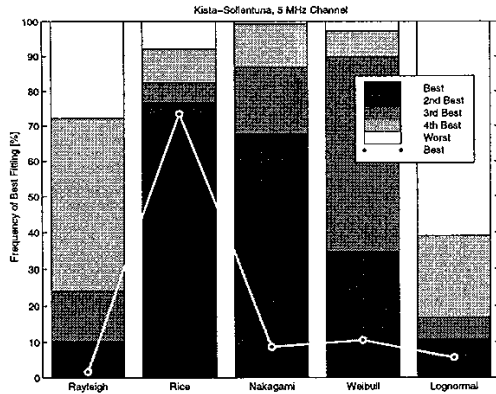

Figure 2. Frequency of best fitting, in the Kramer-von-Mises sense, of empirical distributions to theoretical Rayleigh, Rice, Nakagami, Weibull and Lognormal distributions the 5 MHz channel measured in Kista-Sollentuna.

As is clear from Fig. 2 the best fitting in the Kramer-von-Mises sense, is obtained for the Rice distribution (see Table 1). A similar result was obtained for measurements in Stockholm City. Observe that the Rice distribution includes the Rayleigh probability distribution as a special case.

The frequency of the combination of the best fit and the second best fit of the Nakagami distribution is approximately the same as the frequency of the Rice distribution. This result is probably due to the equivalence of the Rice and the Nakagami probability functions as shown in [9].

4   Global Figures of the Channel and Corresponding Model

In section 3 it was shown that the theoretical Rice probability distribution gives the best fitting to the empirical distribution functions in the Kramer-von-Mises sense. The Rice K-factor was estimated at each delay time for each one of the measured impulse response functions, separately, at Kista-Sollentuna and Stockholm City for the 5 MHz channels. So following the established notations, let us call the plot that show such a dependence Fading Delay Profile (FDP) $K(\tau)$ (see figure 4).

In order to perform simulations that describe the propagation phenomena in appropriate manner it is important to extract most information from measured CIR. It is interesting to know if there is any connection between the channel parameters that could facilitate the reproduc-

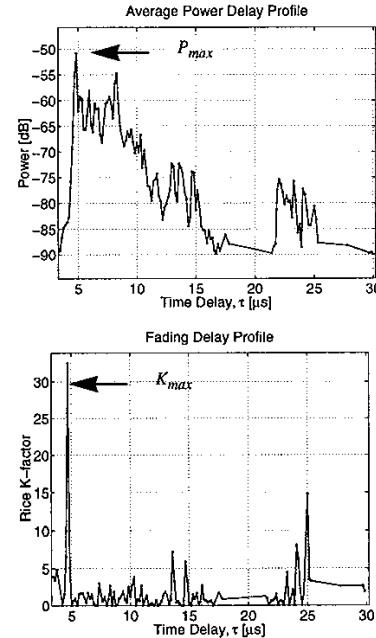tion of the behavior of the channel.

Figure 3.   An example of average Power Delay Profile with corresponding Fading Delay Profile based on 5 MHz channel measurements at the 1.88 GHz band in Stockholm City.

From the average Power Delay Profile (aPDP), obtained from the instantaneous power profiles, the global average Power Delay Profile can be derived in the following way:

$$P_G(\tau) = \left\langle \frac{P(\tau + \tau_{P_{max}})}{P_{tot}} \right\rangle \qquad (4.1)$$

where $<.>$ denotes average over all the measurement locations on a considered propagation area. The strongest multipath component at each aPDP is taken as reference. P_{tot} denotes the total power obtained by integration of $P(\tau)$.

Besides the global aPDP, the global average FDP may also be computed. The global aFDP is defined as follows:

$$K_G(\tau) = \left\langle K(\tau + \tau_{P_{max}}) \right\rangle \qquad (4.2)$$

where $<.>$ is defined above.

Both the global aPDP and the global aFDP for the 5 MHz channels that correspond to Kista-Sollentuna and Stockholm City measurements are shown in Fig. 5. As is clear from those plots, the global aPDP for the Kista-Sollentuna and the Stockholm areas are quite similar. The global aPDP of the Kista-Sollentuna propagation area can be modeled by a single tap at the time delay that corresponds to the strongest tap plus a single-sided exponential decaying function for delays posterior to the first one. In a compact form the function can be expressed by the following equation:

$$P_G(\tau) = \begin{cases} P_0, \tau = \tau_{P_{max}} \\ P_1 e^{-(\tau - \tau_{P_{max}})/\gamma_1}, \tau > \tau_{P_{max}} \end{cases} \quad (4.3)$$

where γ_1 is the time decay constant, P_0, and P_1 are respectively the power level of the strongest peak and the power of the following one. In the same way the global aPDP for Stockholm can also be modeled by the function given by equation (4.3). It is worthwhile to notice that in reality the aPDP for the Stockholm area consists of several clusters (not shown in Fig. 5). Nevertheless, if only power levels over -30 dB are considered, the behavior of the experimental curves can be fitted by function (4.3) alone. Finally, only multipath components incoming at delays $\tau > \tau_{Pmax}$ are considered in model (4.3).

Propagation Area	γ_1 [μs]	(P_0/P_1), [dB]
Kista-Sollentuna	1.3	10
Stockholm City	2.3	15

Table 2   Parameters for the gaPDP model (equation 4.3)

In order to model the dynamic behavior of the channel the correlation between the Rice K-factor in the global aFDP and the power level in the global aPDP was evaluated. It was found that the K-factor at each delay is weakly correlated with the power level at that delay which is clear from Fig. 5. Though, a larger K-factor is observed at the strongest tap. So a possible model for the aFDP could be a tap with a amplitude K_0 at the time delay that corresponds to the strongest tap in the aPDP, and at the following delays taps with equal amplitude K_1. The analytical representation of the model is given:

$$K_G(\tau) = \begin{cases} K_0, \tau = \tau_{P_{max}} \\ K_1, \tau > \tau_{P_{max}} \end{cases} \quad (4.4)$$

where K_0 is the K-factor of the strongest peak (P_0) and K_1 is the K-factor of the following taps (P_1). K_0 and K_1 are given below in Table 3.

K_1 is computed as the average of the K-factors in the aFDP excluding the value corresponding to the strongest tap in the a PDP.

	Kista-Sollentuna 5 MHz channel	Stockholm City 5 MHz channel
K_0	6.5	5.5
K_1	1.4	1.8

Table 3   Parameters for the gaFDP model (equation 4.4)
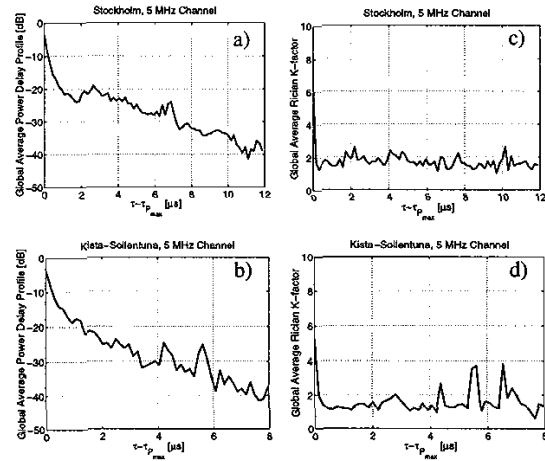

Figure 4.   Global average power delay profiles a)-b) and global average fading delay profiles c)-d) for 5MHz CIR measurement performed in Kista-Sollentuna.
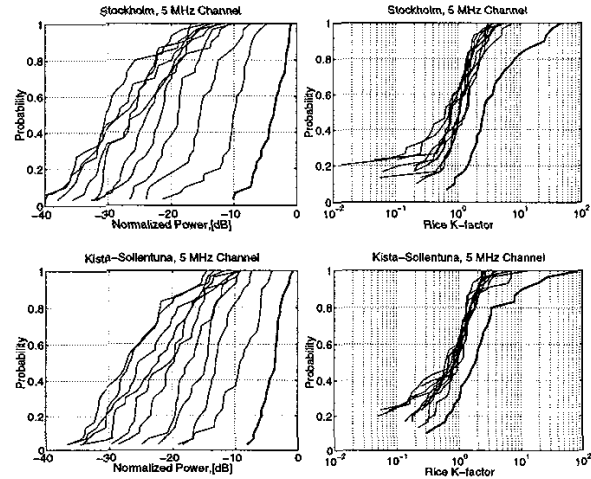

Figure 5.   CPD curves for the eleven first paths shown in Fig. 5. The distributions describe the variation of levels in the PDPs, not the multipath fading variation.

Fig. 6 shows the cumulative probability distribution (CPD) for the power level in the aPDP and the Rice K-factor in the aFDP from which the average profiles (Fig. 5) were derived. From Fig. 6 is clear that those parameter (power level and K-factor) can be assumed lognormal distributed. Further, the variance of the power level corresponding to the strongest multipath is lesser than the variance of the weakest ones, that is the weaker the multipath the larger the variance. On the contrary the variance of the K-factor corresponding to the strongest multipath is larger than the variance of the weakest ones, which have approximately the same magnitude.

5 Summary

In the past sections results from statistical analysis of the fading behavior of multipath components in short-term channel impulse responses have been presented, which can be summarized with the following ideas:

- for the dynamic variation of the multipath amplitudes at a fixed delay, at 1.88 GHz for the 5 MHz channels measured in Kista-Sollentuna and in Stockholm, the theoretical Rice probability distribution gives in most cases (75%) the best fitting in the Kramer-von-Mises sense.

- the global average Power Delay Profile (gaPDP) can be modeled by a single tap at the time delay that corresponds to the strongest tap followed by a single-sided exponential decaying function.

- the fading variation of each channel tap can be characterized by a global average "Fading Delay Profile", that is to each delay in the gaPDP a Rice K-factor is related. The K-factor corresponding to the first and strongest tap in the gaPDP has also the highest value, the following K-factors have a lower value and are all approximately equal.

6 References

[1] G.L.Turin et. al., "A statistical model of urban multipath radio propagation," *IEEE Trans. Veh. Technol.*, vol 21, pp.1-9, 1972

[2] H.Suzuki,"A statistical Model for Urban Radio Propagation," *IEEE Transactions on Communications*, vol. COM-25, pp.637-680, July 1977

[3] W.R. Braun and U. Dersch," A physical model of urban multipath radio propagation,"*IEEE Trans. Veh. Technol.*, vol 40, pp.472-482, 1991

[4] P.C.Fannin, A.Molina, "Analysis of mobile radio channel sounding measurements in inner city Dublin at 1.808 GHz," *IEE Proc.-Commun.*, vol 143, No. 5, pp.311-316, 1996

[5] H.Asplund, A.Alayon Glazunov, J-E.Berg, "An Investigation of Measured and Simulated Wideband Channels with Applications to 1.25 MHz and 5 MHz CDMA Systems," *VTC'98*,Ottawa,May 1998

[6] S.O.Rice, "Mathematical analysis of random noise," *Bell Syst.Tech.J.*,vol.23,pp.282-332,July 1944,and vol.24,pp.46-156,Jan.1945

[7] M.Nakagami, "The m-Distribution-A General Formula of Intensity Distribution of Rapid Fading," inW.C. Hoffman (ed.):*Statistical Methods in Radio Wave Propagation*, London: Pergamon Press,1960.

[8] J. G. Proakis, *Digital Communications*, New York:McGraw-Hill, 1989

[9] S.A.Abbas, A.U.Sheikh "A geometric theory of Nakagami fading multipath mobile radio channel with physical interpretations," IEEE, 1996

[10] A.M.Law, W.D.Kelton, *Simulation Modeling and Analysis*. New York:McGraw-Hill, 1991

[11] R.V.Hogg and E.A.Tanis, *Probability and Statistical Inference*. New York:Macmillan, 1977, pp. 280-285

7 Appendix

The Maximum Likelihood Estimators for the parameters of the Rice distribution (see Table 1 in section 3) are given by the following system of non-linear equations:

$$\begin{cases} 2N\sigma^2 + Ns^2 = \sum_{i=1}^{N} X_i^2 \\ s = \frac{1}{N}\sum_{i=1}^{N} \frac{X_i I_1(X_i s/\sigma^2)}{I_0(X_i s/\sigma^2)} \end{cases} \quad (7.1)$$

where s and σ are the parameters of the Rice distribution, X_i are the experimental sample points with a total of N. $I_0(.)$ and $I_1(.)$ are 0th and 1th order modified Bessel functions of first kind.

The estimate for parameter σ in the Rayleigh distribution is obtained if s is set to zero in the first of equations (7.1).

For the Nakagami distribution, also a system of non-linear equations is obtained for the MLEs:

$$\begin{cases} \Omega = \frac{1}{N}\sum_{i=1}^{N} X_i^2 \\ \ln(m) - \psi(m) = \ln\left(\frac{\frac{1}{N}\sum_{i=1}^{N} X_i^2}{\prod_{i=1}^{N} X_i^{2/N}}\right) \end{cases} \quad (7.2)$$

where Ω and m are the parameters and N and X_i as above. ψ is the digamma function.

Numerical solutions for both equation systems were found by using the Newton-Raphson method.